Effect of Curved Surface of a Shoulder Fillet Round Bar on Stress Concentration Factor for Axial Tension Loading

Hiren Prajapati[a*] & Bhavesh P Patel[b]

[a]Mechanical Engineering Department, Government Engineering College, Modasa, Gujarat, India 383315
[b]Mechanical Engineering Department, U V Patel College of Engineering, Ganpat University, Gujarat, India

*Corresponding author: hirs.mech1985@gmail.com

ABSTRACT

In industries, the shoulder fillet round bar (step shaft) is used to transmit the power and motion to fulfil the requirements of a specific application. A step is provided on the shaft for mounting bearings, sprockets, flywheels, pulleys etc. A step on the round bar behaves as discontinuity. The local stresses developed in the vicinity of the discontinuity, known as stress concentration (SC). The SC is one of the major factors responsible for failure of the mechanical component having discontinuity like step shaft. The shoulder fillet is provided in a step to reduce stress concentration on the shaft. The stress concentration can be measured using the stress concentration factor (SCF). The SCF can be calculated with the help of a fringe pattern. In the present research, experimentally, the fringe pattern was not obtained on the shoulder fillet round bar due to the curved surface of the bar. To overcome this problem, a partial slicing model approach was used. Even though, the obtained fringe patterns were not clear due to the sharp corners present in the partial slicing models. The SCF can be calculated with the help of a fringe pattern. These limitations can be overcome using Finite Element Analysis (FEA) and full slicing approaches. In the present research, the FEA was performed on the flat and curved plate (slice). The Rapport factor (RF) was derived for all possible D/d ratios and determined the effect of a curved surface by finding the equivalent SCF of the shoulder fillet round bar. The FEA results of SCF were validated using the Peterson graph and considered acceptable as per the prevalent industry practices. The present study may help the design engineer to find the minimum SCF for the design of the shoulder fillet round bar for the concerned application. It will reduce the design iterations and chances of failure of the shoulder fillet round bar during its operation.

Keywords: Stress concentration (SC); Stress concentration factor (SCF); Finite Element of Analysis (FEA); Rapport factor (RF); discontinuities; shoulder fillet; flat plate; curve plate

NOTATIONS			ABBREVIATIONS		
K_t	=	Stress concentration factor (unit less)	SC	=	Stress Concentration
σ_{max}	=	Maximum stress (N/mm²)	SCF	=	Stress Concentration Factor
σ_o	=	Nominal stress (N/mm²)	FEA	=	Finite Element Analysis
t	=	Plate thickness (mm)	FDM	=	Fused Deposition Modelling
h	=	Difference between the larger and the smaller radius of the round bar (mm)	BEM	=	Boundary Element Method
D	=	Larger diameter of the round bar and larger width of the plate (mm)	RF	=	Rapport Factor
d	=	Smaller diameter of the round bar and smaller width of the plate (mm)			
P	=	Axial tensile load (N)			

INTRODUCTION

In industries, many unforeseen failures of various parts of machines and equipment have occurred. These failures cause accidents, human injury, and financial losses in many cases of machine and equipment failure. The majority of these failures occur due to different stress raisers present in the machine components like keyways, holes, notches, shoulder fillets, etc. (Norton R. L. 2006). These stress risers are required on the machine components to fulfil their functional requirement but due to their geometrical shape, create localized stresses in the vicinity of discontinuity known as stress concentration (SC). The stress concentration is one of the major factors responsible for the failure of machine components subjected to load. The great challenge for the design engineer is to understand the effect of stress concentration on the function of the machine component based on its geometrical shape and localized loading condition (Shigley J. E et. al. 2008). Thus, stress concentration is a serious issue for design engineers. Stress concentration can be measured by a factor known as the stress concentration factor (SCF). The stress concentration factor (K_t) is the ratio of the maximum stress (σ_{max}) developed in this region to nominal stress (σ_o). Mathematically, SCF can be written as,

$$K_t = \frac{\sigma_{max}}{\sigma_o} \qquad (1)$$

Where,

$\sigma_{nom} = \frac{P}{td}$ For a thin plate element of thickness t and,

$\sigma_{nom} = \frac{4P}{\pi d^2}$ For a circular plate under axial loading

The stress concentration factor (SCF) for a specific geometry can be calculated using the Finite Element Analysis (FEA) approach, theory of elasticity and experimental techniques like the Photoelasticity method (Shigley 2008).

Shoulder fillets are present in many load-bearing structural components and consequently, fillets have been of common interest in the analysis of stress concentrations. The shoulder fillets are provided on a bar or plate to fulfil the functional requirement of the machine, and the component has a sudden change in cross-section. The fillet provided at the shoulder of the round bar or step plate will provide a smooth change in the cross-section and reduce the stress concentration.
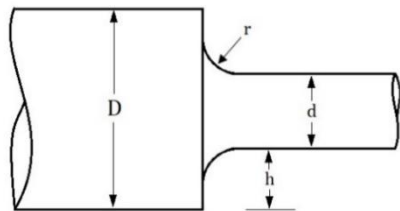

FIGURE 1. The geometry of round bar with shoulder fillet (Sonmez 2009)

Figure 1 shows a shaft with a shoulder fillet (Sonmez F O 2009). Shoulder fillets are ever-present in many load-bearing structural components and consequently, fillets have been of common interest in the analysis of stress concentrations. The shoulder fillets are provided on a bar or plate to fulfil the functional requirement of the machine, and the component has a sudden change in cross-section. The fillet radius provided at the shoulder of the round bar or step plate, will provide a smooth change in cross-section and reduce the stress concentration. Selection of different parameters like fillet radius r, diameters (D, d) and its ratios D/d, r/d are based on the Peterson handbook (Pilkey 1997).
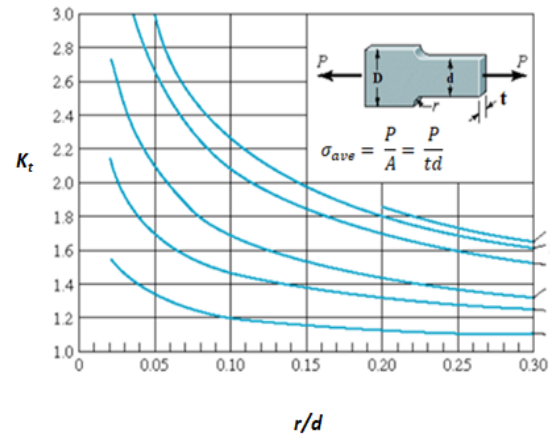

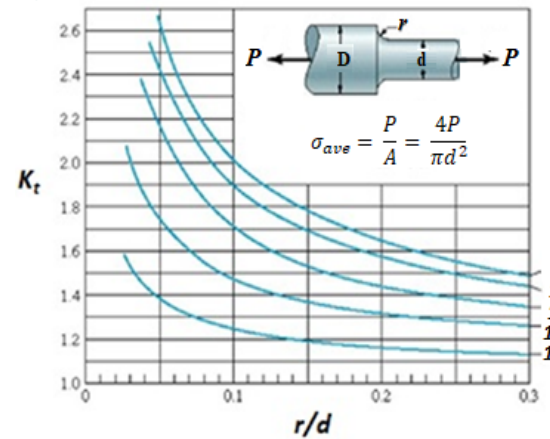FIGURE 2. Stress concentration factor for fillets in the flat plate (Collins J A, 1981)

FIGURE 3. Stress concentration factor for fillets in the round bar (Collins 1981)

Figure 2 shows the effect of the ratio *r/d* on the stress concentration factor (K_t) for the shoulder fillet plate. From Figure 2, it is depicted that the smaller the fillet radius (r) or larger the D/d ratio, results in higher SCF. One can find the stress concentration factor (K_t) from graphs presented in Figure 2 and Figure 3 concerning the r/d ratio for particular D/d ratio of flat plate and round bar respectively. In the present study, the notations used are considered common for flat plates, curved plates and round bars to eliminate the confusion, complexity and ease of validation. The slice

(plate) with curvature at the thickness section of the flat plate is termed a curved plate.

In the present research, it is difficult to find the stress concentration factor for shoulder fillet round bar using an experimental set-up i.e. Photoelastic apparatus. In the experimental approach, the fringe pattern is not visible due to the curved surface of the round bar and not possible to count the number of fringes on the curved surface. The stress concentration factor can be calculated using fringes obtained from experimentation. To overcome this problem, the slicing approach was adopted along with the Finite Element Analysis approach. The authors have made efforts to determine the effect of the curvature of a curved plate in comparison with a flat plate and the rapport factor derived as multiplying factor. The rapport factor helps to determine the equivalent SCF for a round bar. The experimental work can be avoided to determine the SCF of the shoulder fillet round bar. The results were validated with the help of available literature. A detailed description of problem formulation is given in sections.

RELATED LITERATURE REVIEW

The shaft is a critical component used in different applications to transmit power and motion from one machine to another. To fulfil the functional requirement, sudden changes in cross-section (shoulder), keyway, groove/notches, etc. provided to the shaft (round bar) are called discontinuities. These discontinuities create localized stresses known as stress concentration. The majority of failure of the shaft is due to stress concentration. To avoid this problem, it is important to consider the effect of stress concentration during the design of the shaft. Many researchers have contributed their time and effort to understanding the effect of stress concentration due to discontinuities present in the components. Researchers have reported their observations and research outcomes for various discontinuities like keyway (Pilkey W D 1997; Pedersen 2010; Ajovalasit et al. 2014), fillet (Sonmez F O 2009; Hartman J B et al. 1950; Allison I M 1961; Pilkey W D 1997; Zappalorto M et al. 2008; Muminovic A J 2016; Ajovalasit A et al. 2014; Pedersen N L 2018; Sorrentino A et al. 2019), grooves/notches (Pilkey W D 1997; Zappalorto M et al. 2008; Taylor D et al. 2011; Muminovic A J 2016; Zappalorto M et al. 2014), hole (Muminovic A J 2016; Pedersen N L 2019; Ashish 2020; Ouali O 2021) etc. The different types of loads were considered for their study to observe the effect of stress concentration on the components due to the presence of discontinuities. The tensile load (Allison I M 1961; Pilkey W D 1997; Pedersen N L 2010; Zappalorto M et al. 2008; Muminovic A J 2016; Zappalorto M et al. 2014; Pedersen N L 2018; Xiong Z 2021), bending load (Hartman J B et al. 1950; Allison I M 1961; Pilkey W D 1997; Muminovic A J 2013; Pedersen N L 2018; Gyoko O 2020), torsion load (Allison I M 1961; Pilkey W D 1997; Muminovic A J 2013; Ajovalasit et al. 2018; Pedersen 2018), combined load (Sonmez F O 2009; Muminovic A J 2013; Pedersen N L 2018), and uniaxial and biaxial loading (Ashish 2020;

Ouali O M 2021; Xiong Z 2021) considered by the various researchers and found the stress concentration factor under these loading conditions for different discontinuities. Different methods were applied to determine the stress concentration factor-like Finite Element Method (FEM) (Pedersen N L 2010; Zappalorto M et al. 2008; Taylor D et al. 2011; Muminovic A J 2016; Zappalorto M et al. 2014; Ajovalasit A et al. 2014; Pedersen N L 2018; Pedersen N L 2019; Sorrentino A et al. 2019; Ouali O M 2021; Xiong Z 2021), analytical method (Pedersen N L 2010; Zappalorto M et al. 2008; Taylor D et al. 2011; Ashish 2020; Ouali O M 2021; Ding M 2021) and experimental method (Ajovalasit A et al. 2014; Gyoko O 2020) for different discontinuities with different loading conditions. Few authors have studied shape optimization to reduce stress concentration (Pedersen 2010; Pedersen 2019; Sorrentino 2019). Augusto Ajovalasit et al. used the Fused Deposition Modelling (FDM) and Boundary Element Method (BEM) along with the Finite Element Method (FEM) and determined the SCF for shaft having keyway and shoulder fillet under the torsional loading condition. The obtained results from the numerical method were compared with the existing lectures and experimental work to validate the results obtained by them (Ajovalasit et al. 2014). The majority of researchers have used the FEM and analytical methods, whereas very few researchers have adopted the experimental method to determine the SCF for different components having different discontinuities. In the present research, the authors have applied the experimental method to determine the SCF of shoulder filleted round bar (shaft) under tensile loading and the limitations of experimental work were eliminated using partial and full-slicing approaches using the FEA method. The validation of work was given using the existing standard Peterson's graph. The % variation in the results was presented and found that the % variations in the results of SCF are acceptable as per current industrial practices.

PROBLEM FORMULATION AND MOTIVATION

Within the referred literature, it is found that many researchers have worked on the determination of stress constriction for different discontinuities present in the component using the FEA approach. It is found that from the literature review, the experimental work was performed for discontinuities like key-way and groove on the round bar, fillet and notches on a plate. Peterson generated the SCF curves using available experimental data for the shoulder fillet round bar. These experimental data were developed by other researchers and used by Peterson to determine the SCF for the shoulder fillet round bar. The information regarding the performed experimental work and obtained experimental results were not mentioned in any available literature within the referred literature review. The authors got the motivation to perform the experimental work on the shoulder fillet round bar to determine the SCF. Figures 4 (a) and (b) show the test specimen prepared before and after the buffing operation, respectively.

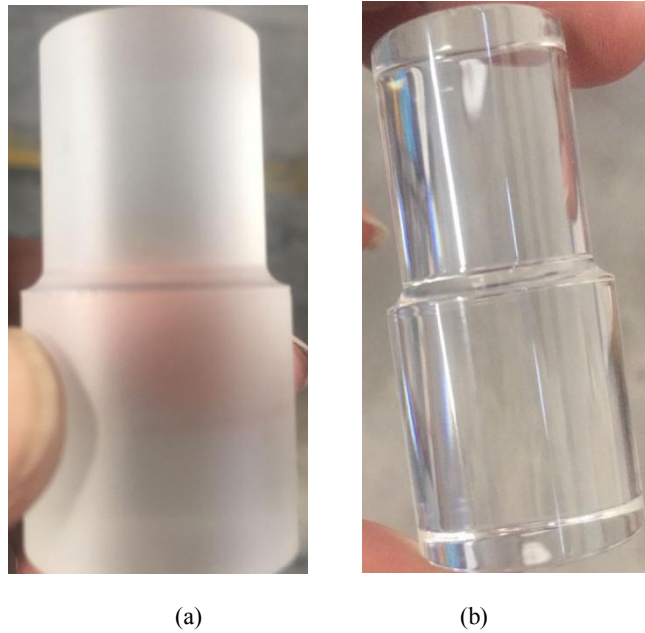(a)   (b)

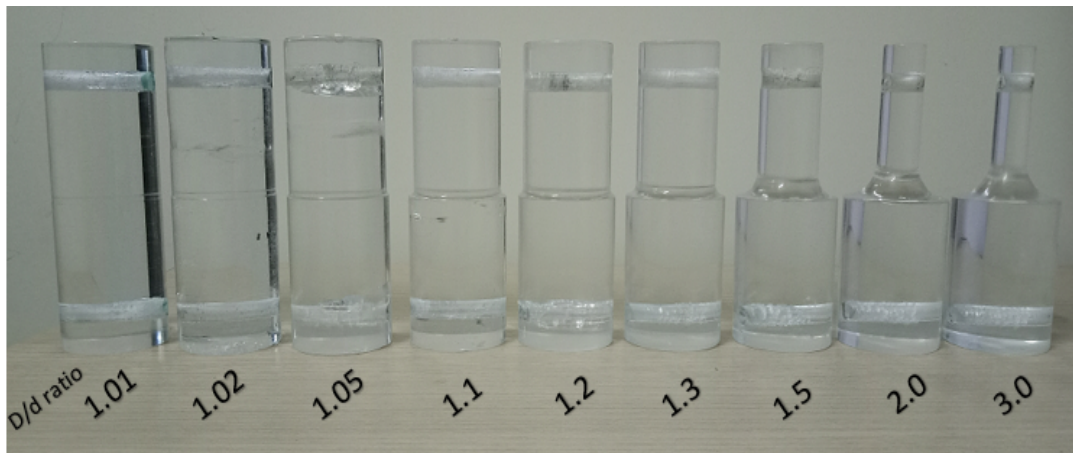FIGURE 4. Test specimen (a) before buffing operation and (b) after buffing operation.

FIGURE 5. Test specimens after buffing operation for all D/d ratios.

Test specimens were prepared using a polycarbonate rod by performing turning and buffing operations on it concerning standard D/d ratios available in the design data book (PSG Design data 2010) (see Figure 5). Figure 6 shows the experimental setup known as Photoelastic apparatus with taxonomies. The experiments were conducted on photoelastic apparatus. It was customized for a load-carrying capacity of 1 kN with a digital load indicator (tension, compression and torsion). Here, the scope of the proposed experimental work is limited to tensile load only.
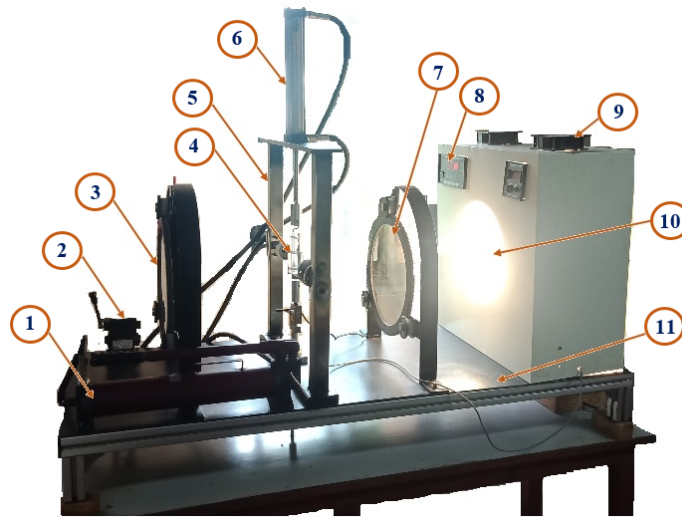
1. Hydraulic pump 2. One directional valve 3. Circular polariscope 4. Test specimen 5. Mechanical load frame 6. Hydraulic cylinder 7. Circular analyzer 8. Digital load indicator 9. Cooling fan 10. Monochromatic and white light source 11. Levelling table

FIGURE 6. Experimental setup-Photoelastic apparatus.

It was not possible to generate the fringe pattern on the round bar due to the covered surface of the round bar. It is very clear from Figure 7 that the fringe pattern is not visible under applied tension loading. To overcome this problem, one side partial slicing approach was adopted and prepared the workpiece accordingly.

FIGURE 7. Image of the shouldered shaft under axial tension on photoelastic apparatus.

Figures 8 (a) and (b) show the partial slicing from one side and both sides of the specimen [6-9]. Even though, the fringes were not visible on the round bar due to the narrow portion of the shoulder fillet of the round bar, as shown in Figure 8 (a). The buffing operation was not possible in the narrow portion of the shoulder fillet to prepare the workpiece for experimentation. Still, fringes were not visible on the one side partially sliced workpiece prepared. Again, to overcome this problem, the authors have applied the two side partial slicing approach to preparing the workpiece as shown in Figure 8 (b).
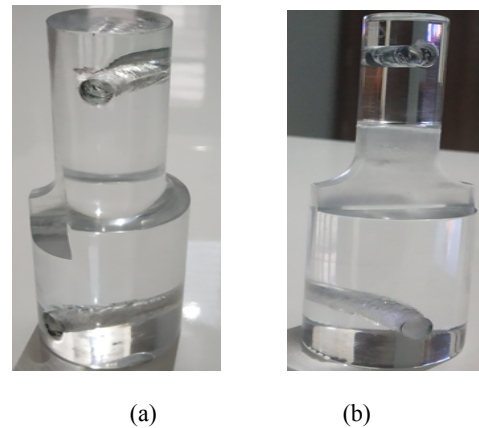

(a)   (b)

FIGURE 8. (a) Partial slicing from one side and (b) Partial slicing from both sides.

Even though, the fringes were not visible on the workpiece. The curved surface plate was not possible to manufacture due to the limitation of generation of the curve with the required radius on a plate or to cut the slice with a curved portion from the shoulder fillet round bar.

Authors have adopted the FEA approach with full sliced flat plates with different thicknesses. The stress concentration factor was determined using the FEA approach and derived rapport factor. The rapport factor is the multiplying factor that considers the effect of curvature present on the curved plate compared to the flat plate and is used to determine the equivalent SCF of the shoulder fillet round bar. The use of the rapport factor eliminates the experimental work.

METHODOLOGY

Ten different 3D models of a flat plate (Figure 9 (a)) and curved plate (Figure 9 (b)) were developed by varying the thickness of the plate from 4 mm to 40 mm in the interval of 4 mm (i.e. 4 mm, 8 mm, 12 mm…., 40 mm) for all possible D/d ratios as per PSG design data book.
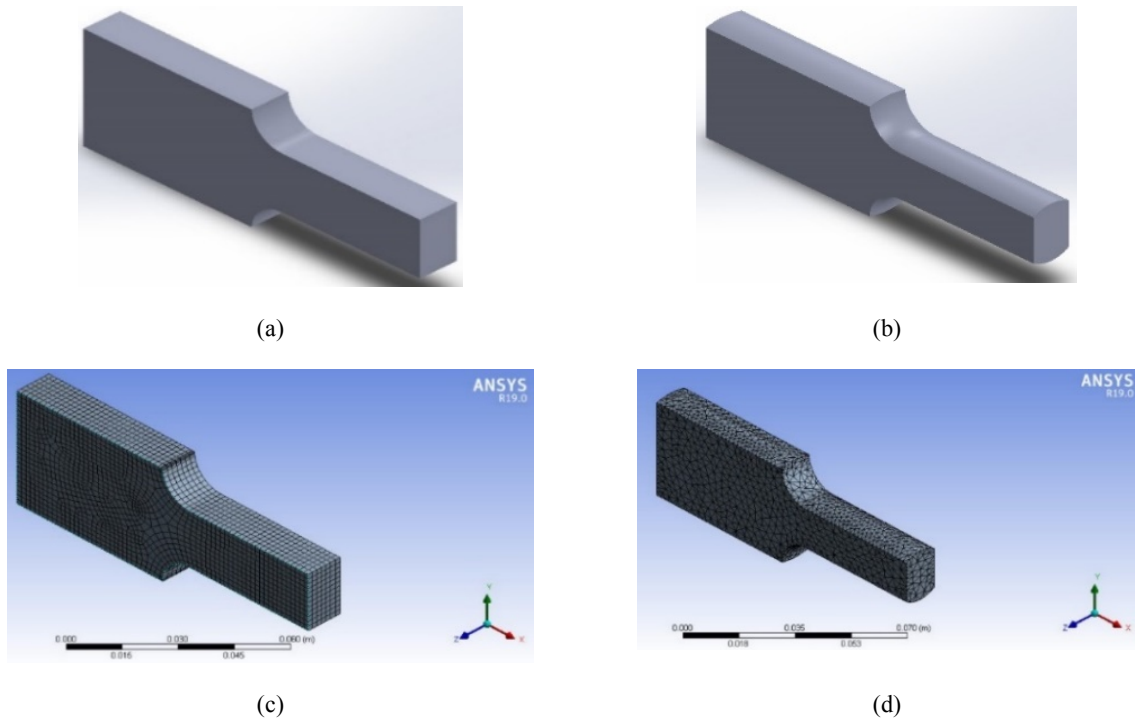

(a)

(b)

(c)

(d)

FIGURE 9. 3D model and meshed model of slicing of round bar (a) flat plate and (b) curved plate (c) meshed model of a flat plate (d) meshed model of a curved plate

All 3D models were prepared using Solid works 16.0. The FEA was performed using ANSYS 19.0 software. Figure 9 (c) and Figure 9 (d) show the meshed model of flat and curved plates, respectively. The boundary conditions and uniaxial tension loading are applied as presented in Figure 10.
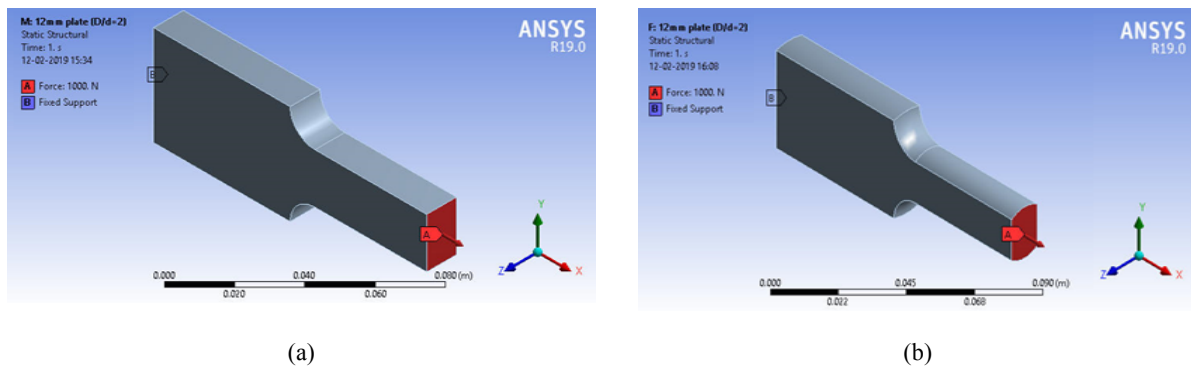

(a)

(b)

FIGURE 10. Loading and boundary conditions for axial tension loading (a) flat plate and (b) curved plate.

The standard methodology was adopted to perform the FEA as per prevalent industrial practices. The effect of the curvature on a curved plate was determined by conducting a comparison with a flat plate of the same thickness. The FEA was performed for all models with different D/d ratios (i.e. 1.01 to 3.0). EN31 is a linear elastic material, and it is taken as a workpiece material. EN31 is widely used as plate and shaft material for different industrial applications. The properties of the EN31 material are tabulated in Table 1. Equivalent (von Mises) stress is calculated from the FEA results for all the slice models.

TABLE 1. Material properties of EN31 [10]

Property	Value	Unit
Density	7600	Kg/m^3
Isotropic properties		
Young's modulus	207	MPa
Poisson's ratio	0.3	--
Bulk modulus	172.5	GPa
Shear modulus	80	GPa
Tensile yield strength	460	MPa
Tensile ultimate strength	560	MPa

The magnitude of the tensile load (i.e. 1000 N) is considered based on the feasible load range applied through the experimental setup (i.e. Photoelastic apparatus). The workpiece may get failure or bend beyond the load of 1000 N applied experimentally. The constant uniaxial tensile load of 1000 N is applied on one end of the plate for all FEA iterations with different D/d ratios. However, for brevity and simplicity of presentation in the paper, only one D/d ratio (i.e. D/d = 2) is considered for comparison. The von Mises stresses obtained from FEA were compared for flat plats and curved plates having a thickness of 4 mm to 40 mm in the interval of 4 mm plate thickness. For checking mesh convergence, element size was reduced, and change in results was obtained within 1% compared to element size considered in the analysis reflecting the adequacy of the mesh size.
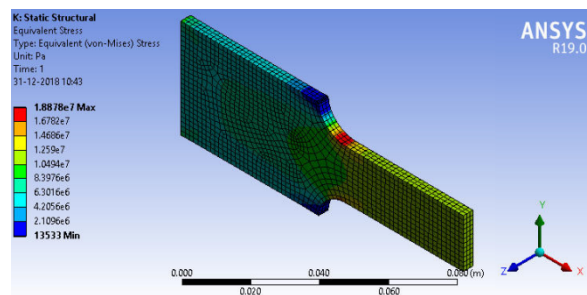
(a) 4 mm thickness of the flat plate
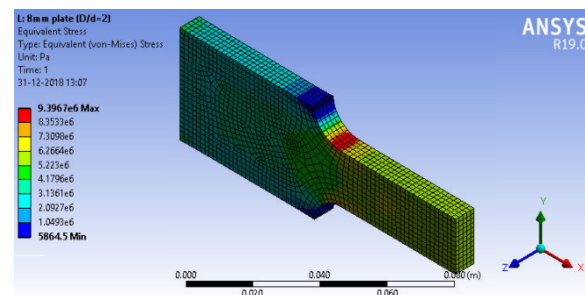
(b) 8 mm thickness of the flat plate
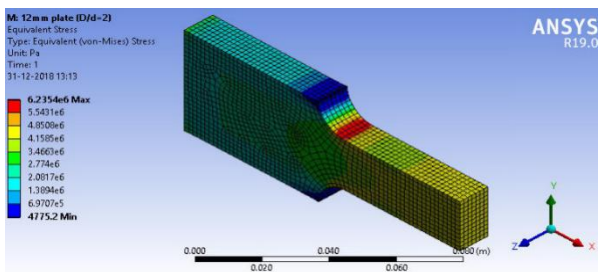
(c) 12 mm thickness of the flat plate

(d) 16 mm thickness of the flat plate

(e) 20 mm thickness of the flat plate

(f) 24 mm thickness of the flat plate
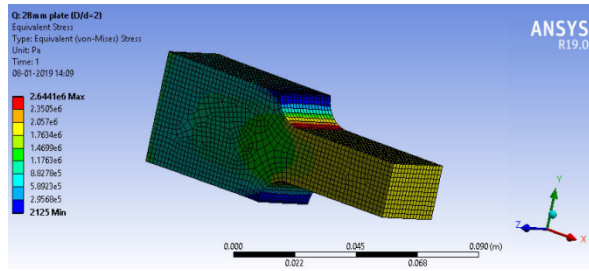
(g) 28 mm thickness of the flat plate
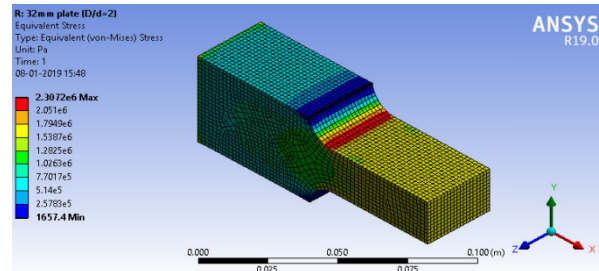
(h) 32 mm thickness of the flat plate
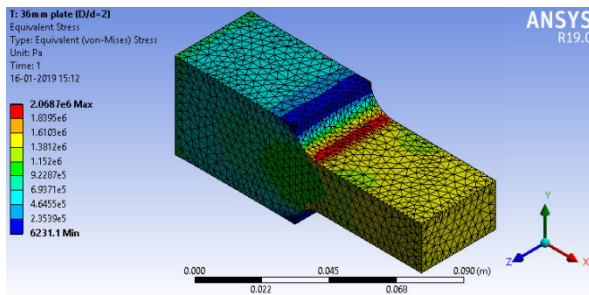
(i) 36 mm thickness of the flat plate
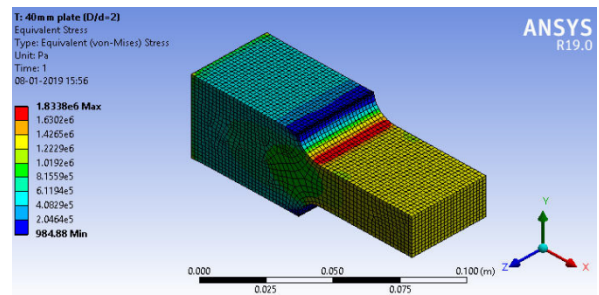
(j) 40 mm thickness of the flat plate

FIGURE 11. Equivalent (von Mises) stress for D/d = 2 (D = 40 mm and d = 20 mm) – flat plate.

Figure 11 shows the FEA results of a flat plate with D/d = 2, having plate thickness from 4 mm to 40 mm with an interval of 4 mm plate thickness under axial tension loading. The same procedure was repeated for the curve plate.
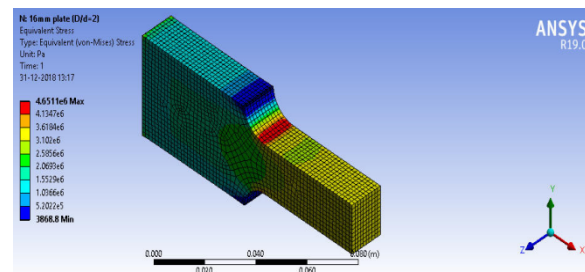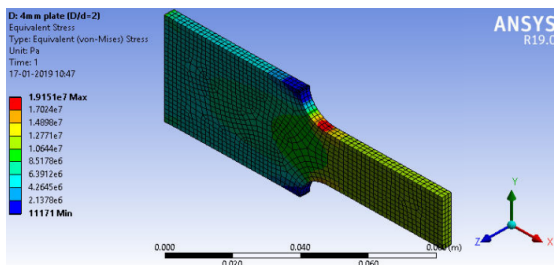

(a) 4 mm thickness of the curved plate
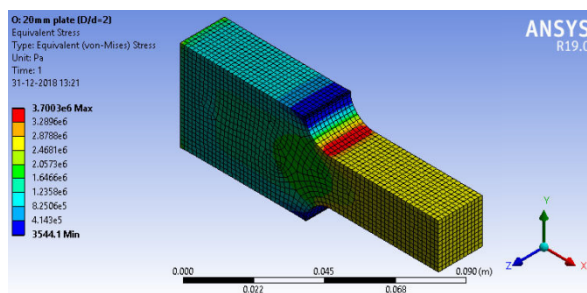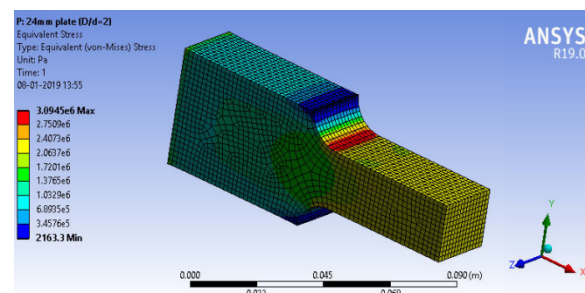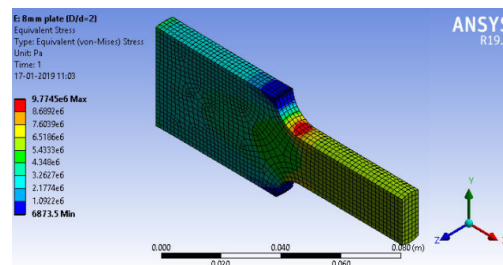

(b) 8 mm thickness of the curved plate

(c) 12 mm thickness of the curved plate

(d) 16 mm thickness of the curved plate

(e) 20 mm thickness of the curved plate
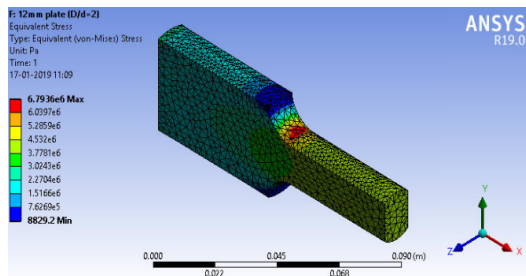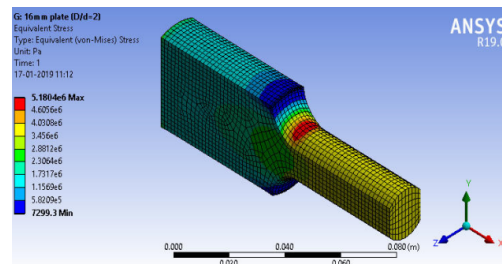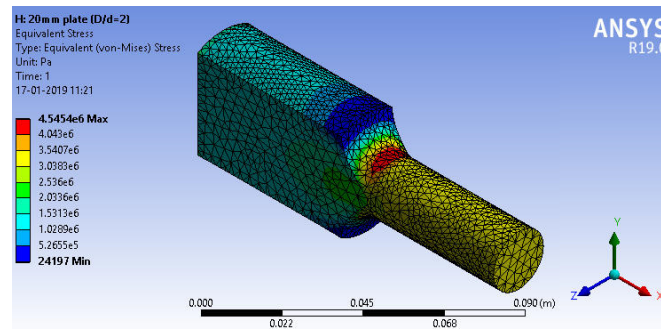
FIGURE 12. Equivalent (von Mises) stress for D/d = 2 (D = 40 mm and d = 20 mm) - curved plate.

The FEA results for equivalent (von Mises) stress for curved plate with D/d ratio of 2 presented in the Figure 12. Similarly, FEA was carried out on flat plates and curved plates for all the D/d ratios (i.e. D/d = 1.01, D/d = 1.02, D/d = 1.05, D/d = 1.1, D/d = 1.2, D/d = 1.3, D/d = 1.5, D/d = 2.0, D/d = 3) and results were obtained in terms of SCF. The results are tabulated in the Table 2 to Table 10 for different D/d ratios.

RESULTS AND DISCUSSION

In the present work, the authors have identified the effect of the curvature of a curved plate in comparison with a flat plate by performing FEA. This effect of the curvature will give an equivalent magnitude of SCF compared to a round bar, and it is termed a rapport factor. The rapport factor is a multiplying factor with the SCF of a flat plate. It gives the equivalent SCF of the round bar. Table 2 to Table 10 shows the Equivalent (von Mises) stress, SCF for flat and curved plates, Rapport factor for SCF, Equivalent SCF for a round bar and SCF obtained from Peterson graph for different D/d ratios (i.e. D/d = 1.01, D/d = 1.02, D/d = 1.05, D/d = 1.1, D/d = 1.2, D/d = 1.3, D/d = 1.5, D/d = 2.0, D/d = 3). The h= r is considered for optimum SCF based on the Peterson data of SCF and the literature available (Bhavesh et al. 2018). In the present case, the notations used are common for flat plates and round bars for simplifying the results and validation purposes.

TABLE 2. SCF for a flat plate, a curved plate, the rapport factor for SCF, the equivalent SCF for a round bar and the SCF from the Peterson graph under axial tension loading for D/d = 1.01.

D (mm)	d (mm)	D/d	h (mm)	r (mm)	Thickness t (mm)	Equivalent (von Mises) stress (MPa)	SCF for flat plate	SCF for curved plate	Rapport factor for SCF	Equivalent SCF for round bar	SCF from Peterson graph
40	39.6	1.01	0.20	0.20	4.000	11.652	1.85	1.81	0.934	1.72	
40	39.6	1.01	0.20	0.20	8.000	6.2928	1.99	1.97	0.934	1.86	
40	39.6	1.01	0.20	0.20	12.000	4.4249	2.10	2.11	0.934	1.96	
40	39.6	1.01	0.20	0.20	16.000	3.5048	2.22	2.19	0.934	2.07	
40	39.6	1.01	0.20	0.20	20.000	2.8988	2.30	2.28	0.934	2.15	1.94
40	39.6	1.01	0.20	0.20	24.000	2.4619	2.34	2.36	0.934	2.19	
40	39.6	1.01	0.20	0.20	28.000	2.163	2.40	1.95	0.934	2.24	
40	39.6	1.01	0.20	0.20	32.000	1.9499	2.47	2.03	0.934	2.31	
40	39.6	1.01	0.20	0.20	36.000	1.7792	2.54	2.08	0.934	2.37	
40	39.6	1.01	0.20	0.20	40.000	1.6287	2.58	---	0.934	2.41	

TABLE 3. SCF for a flat plate, a curved plate, the rapport factor for SCF, the equivalent SCF for a round bar and the SCF from the Peterson graph under axial tension loading for D/d = 1.02.

D (mm)	d (mm)	D/d	h (mm)	r (mm)	Thickness t (mm)	Equivalent (von Mises) stress (MPa)	SCF for flat plate	SCF for curved plate	Rapport factor for SCF	Equivalent SCF for round bar	SCF from Peterson graph
40	39.21	1.02	0.40	0.40	4.000	11.586	1.82	1.78	0.933	1.70	
40	39.21	1.02	0.40	0.40	8.000	6.3224	1.98	1.95	0.93	1.85	
40	39.21	1.02	0.40	0.40	12.000	4.4659	2.10	2.08	0.93	1.96	
40	39.21	1.02	0.40	0.40	16.000	3.5065	2.20	2.16	0.93	2.05	
40	39.21	1.02	0.40	0.40	20.000	2.914	2.29	2.25	0.93	2.13	
40	39.21	1.02	0.40	0.40	24.000	2.4845	2.34	2.33	0.93	2.18	2.00
40	39.21	1.02	0.40	0.40	28.000	2.1947	2.41	1.98	0.93	2.25	
40	39.21	1.02	0.40	0.40	32.000	1.965	2.47	2.07	0.93	2.30	
40	39.21	1.02	0.40	0.40	36.000	1.7804	2.51	2.06	0.93	2.35	
40	39.21	1.02	0.40	0.40	40.000	1.6321	2.56	---	0.93	2.39	

TABLE 4. SCF for a flat plate, a curved plate, the rapport factor for SCF, the equivalent SCF for a round bar and the SCF from the Peterson graph under axial tension loading for D/d = 1.05.

D (mm)	d (mm)	D/d	h (mm)	r (mm)	Thickness t (mm)	Equivalent (von Mises) stress (MPa)	SCF for flat plate	SCF for curved plate	Rapport factor for SCF	Equivalent SCF for round bar	SCF from Peterson graph
40	38.095	1.05	0.95	0.95	4.00	11.688	1.781	1.74	0.937	1.67	
40	38.095	1.05	0.95	0.95	8.00	6.31	1.923	1.90	0.937	1.80	
40	38.095	1.05	0.95	0.95	12.00	4.4367	2.028	2.02	0.937	1.90	
40	38.095	1.05	0.95	0.95	16.00	3.509	2.138	2.09	0.937	2.00	
40	38.095	1.05	0.95	0.95	20.00	2.8894	2.201	2.19	0.937	2.06	
40	38.095	1.05	0.95	0.95	24.00	2.4695	2.257	2.25	0.937	2.12	2.02
40	38.095	1.05	0.95	0.95	28.00	2.1695	2.314	1.92	0.937	2.17	
40	38.095	1.05	0.95	0.95	32.00	1.9559	2.384	2.02	0.937	2.23	
40	38.095	1.05	0.95	0.95	36.00	1.7664	2.422	2.01	0.937	2.27	
40	38.095	1.05	0.95	0.95	40.00	1.6181	2.465	----	0.937	2.31	

TABLE 5. SCF for a flat plate, a curved plate, the rapport factor for SCF, the equivalent SCF for a round bar and the SCF from the Peterson graph under axial tension loading for D/d = 1.1.

D (mm)	d (mm)	D/d	h (mm)	r (mm)	Thickness t (mm)	Equivalent (von Mises) stress (MPa)	SCF for flat plate	SCF for curved plate	Rapport factor for SCF	Equivalent SCF for round bar	SCF from Peterson graph
40	36.36	1.10	1.82	1.82	4.00	11.929	1.735	1.73	0.991	1.72	
40	36.36	1.10	1.82	1.82	8.00	6.304	1.833	1.86	0.991	1.82	
40	36.36	1.10	1.82	1.82	12.00	4.4657	1.948	1.92	0.991	1.93	
40	36.36	1.10	1.82	1.82	16.00	3.5115	2.042	2.00	0.991	2.02	
40	36.36	1.10	1.82	1.82	20.00	2.9104	2.116	2.09	0.991	2.10	
40	36.36	1.10	1.82	1.82	24.00	2.5083	2.188	2.17	0.991	2.17	1.89
40	36.36	1.10	1.82	1.82	28.00	2.1986	2.238	2.33	0.991	2.22	
40	36.36	1.10	1.82	1.82	32.00	1.9709	2.293	2.44	0.991	2.27	
40	36.36	1.10	1.82	1.82	36.00	1.7806	2.330	2.00	0.991	2.31	
40	36.36	1.10	1.82	1.82	40.00	1.6287	2.368	---	0.991	2.35	

TABLE 6. SCF for a flat plate, a curved plate, the rapport factor for SCF, the equivalent SCF for a round bar and the SCF from the Peterson graph under axial tension loading for D/d = 1.2.

D (mm)	d (mm)	D/d	h (mm)	r (mm)	Thickness t (mm)	Equivalent (von Mises) stress (MPa)	SCF for flat plate	SCF for curved plate	Rapport factor for SCF	Equivalent SCF for round bar	SCF from Peterson graph
40	33.33	1.20	3.34	3.34	4.00	11.795	1.573	1.677	1.166	1.83	
40	33.33	1.20	3.34	3.34	8.00	5.8203	1.552	1.7547	1.166	1.81	
40	33.33	1.20	3.34	3.34	12.00	3.8502	1.540	1.7630	1.166	1.80	
40	33.33	1.20	3.34	3.34	16.00	2.867	1.529	1.7649	1.166	1.78	
40	33.33	1.20	3.34	3.34	20.00	2.2879	1.525	1.7950	1.166	1.78	
40	33.33	1.20	3.34	3.34	24.00	1.7579	1.406	1.7915	1.166	1.64	1.79
40	33.33	1.20	3.34	3.34	28.00	1.5798	1.474	1.6889	1.166	1.72	
40	33.33	1.20	3.34	3.34	32.00	1.2238	1.305	1.6111	1.166	1.52	
40	33.33	1.20	3.34	3.34	36.00	1.154	1.385	---	---	---	
40	33.33	1.20	3.34	3.34	40.00	1.0411	1.388	---	---	---	

TABLE 7. SCF for a flat plate, a curved plate, the rapport factor for SCF, the equivalent SCF for a round bar and the SCF from the Peterson graph under axial tension loading for D/d = 1.3.

D (mm)	d (mm)	D/d	h (mm)	r (mm)	Thickness t (mm)	Equivalent (von Mises) stress (MPa)	SCF for flat plate	SCF for curved plate	Rapport factor for SCF	Equivalent SCF for round bar	SCF from Peterson graph
40	30.76	1.30	4.62	4.62	4.00	15.052	1.852	1.881	0.985	1.82	
40	30.76	1.30	4.62	4.62	8.00	7.4387	1.831	1.849	0.985	1.80	
40	30.76	1.30	4.62	4.62	12.00	4.919	1.816	1.819	0.985	1.79	
40	30.76	1.30	4.62	4.62	16.00	3.658	1.800	1.773	0.985	1.77	
40	30.76	1.30	4.62	4.62	20.00	2.9166	1.794	1.791	0.985	1.77	
40	30.76	1.30	4.62	4.62	24.00	2.4759	1.828	1.708	0.985	1.80	1.83
40	30.76	1.30	4.62	4.62	28.00	2.1749	1.873	1.772	0.985	1.84	
40	30.76	1.30	4.62	4.62	32.00	1.9605	1.930	---	---	---	
40	30.76	1.30	4.62	4.62	36.00	1.7794	1.970	---	---	---	
40	30.76	1.30	4.62	4.62	40.00	1.638	2.015	---	---	---	

TABLE 8. SCF for a flat plate, a curved plate, the rapport factor for SCF, the equivalent SCF for a round bar and the SCF from the Peterson graph under axial tension loading for D/d = 1.5.

D (mm)	d (mm)	D/d	h (mm)	r (mm)	Thickness t (mm)	Equivalent (von Mises) stress (MPa)	SCF for flat plate	SCF for curved plate	Rapport factor for SCF	Equivalent SCF for round bar	SCF from Peterson graph
40	26.67	1.50	6.67	6.67	4.00	16.472	1.7572	1.68	1.067	1.88	
40	26.67	1.50	6.67	6.67	8.00	8.1656	1.7422	1.78	1.067	1.86	
40	26.67	1.50	6.67	6.67	12.00	5.3999	1.7282	1.78	1.067	1.84	
40	26.67	1.50	6.67	6.67	16.00	4.0093	1.7108	1.84	1.067	1.83	
40	26.67	1.50	6.67	6.67	20.00	3.1918	1.7025	1.94	1.067	1.82	
40	26.67	1.50	6.67	6.67	24.00	2.6086	1.6697	1.97	1.067	1.78	1.79
40	26.67	1.50	6.67	6.67	28.00	2.286	1.7071	---	---	---	
40	26.67	1.50	6.67	6.67	32.00	2.006	1.7120	---	---	---	
40	26.67	1.50	6.67	6.67	36.00	1.8056	1.7336	----	---	---	
40	26.67	1.50	6.67	6.67	40.00	1.634	1.7432	---	----	---	

TABLE 9. SCF for a flat plate, a curved plate, the rapport factor for SCF, the equivalent SCF for a round bar and the SCF from the Peterson graph under axial tension loading for D/d = 2.

D (mm)	d (mm)	D/d	h (mm)	r (mm)	Thickness t (mm)	Equivalent (von Mises) stress (MPa)	SCF for flat plate	SCF for curved plate	Rapport factor for SCF	Equivalent SCF for round bar	SCF from Peterson graph
40	20	2.00	10	10	4.00	18.878	1.5102	1.53	1.097	1.66	
40	20	2.00	10	10	8.00	9.3967	1.5035	1.56	1.097	1.65	
40	20	2.00	10	10	12.00	6.2354	1.4965	1.63	1.097	1.64	
40	20	2.00	10	10	16.00	4.6511	1.4884	1.66	1.097	1.63	
40	20	2.00	10	10	20.00	3.7003	1.4801	1.82	1.097	1.62	
40	20	2.00	10	10	24.00	3.9045	1.8742	---	---	---	---
40	20	2.00	10	10	28.00	2.644	1.4806	---	---	---	
40	20	2.00	10	10	32.00	2.3072	1.4766	---	---	---	
40	20	2.00	10	10	36.00	2.0687	1.4895	---	---	---	
40	20	2.00	10	10	40.00	1.8338	1.4670	---	---	---	

TABLE 10. SCF for a flat plate, a curved plate, the rapport factor for SCF, the equivalent SCF for a round bar and the SCF from the Peterson graph under axial tension loading for D/d = 3.

D (mm)	d (mm)	D/d	h (mm)	r (mm)	Thickness t (mm)	Equivalent (von Mises) stress (MPa)	SCF for flat plate	SCF for curved plate	Rapport factor for SCF	Equivalent SCF for round bar	SCF from Peterson graph
40	13.33	3	13.34	13.34	4.00	23.806	1.2693	1.38	1.109	1.41	
40	13.33	3	13.34	13.34	8.00	12.123	1.2928	1.38	1.109	1.43	
40	13.33	3	13.34	13.34	12.00	7.9838	1.2771	1.50	1.109	1.42	
40	13.33	3	13.34	13.34	16.00	5.9876	1.2770	---	---	---	
40	13.33	3	13.34	13.34	20.00	4.7989	1.2794	---	---	---	
40	13.33	3	13.34	13.34	24.00	3.9779	1.2726	---	---	---	---
40	13.33	3	13.34	13.34	28.00	3.4193	1.2762	---	---	---	
40	13.33	3	13.34	13.34	32.00	2.9713	1.2674	---	---	---	
40	13.33	3	13.34	13.34	36.00	2.6184	1.2565	---	---	---	
40	13.33	3	13.34	13.34	40.00	2.3404	1.2479	---	---	---	

From Table 2 to Table 10, it is clear that for a particular D/d ratio, the value of the r/d ratio is constant. The Peterson curve represents the relations between the D/d ratio, r/d ratio and stress concentration factor (K_t) for a flat plate.
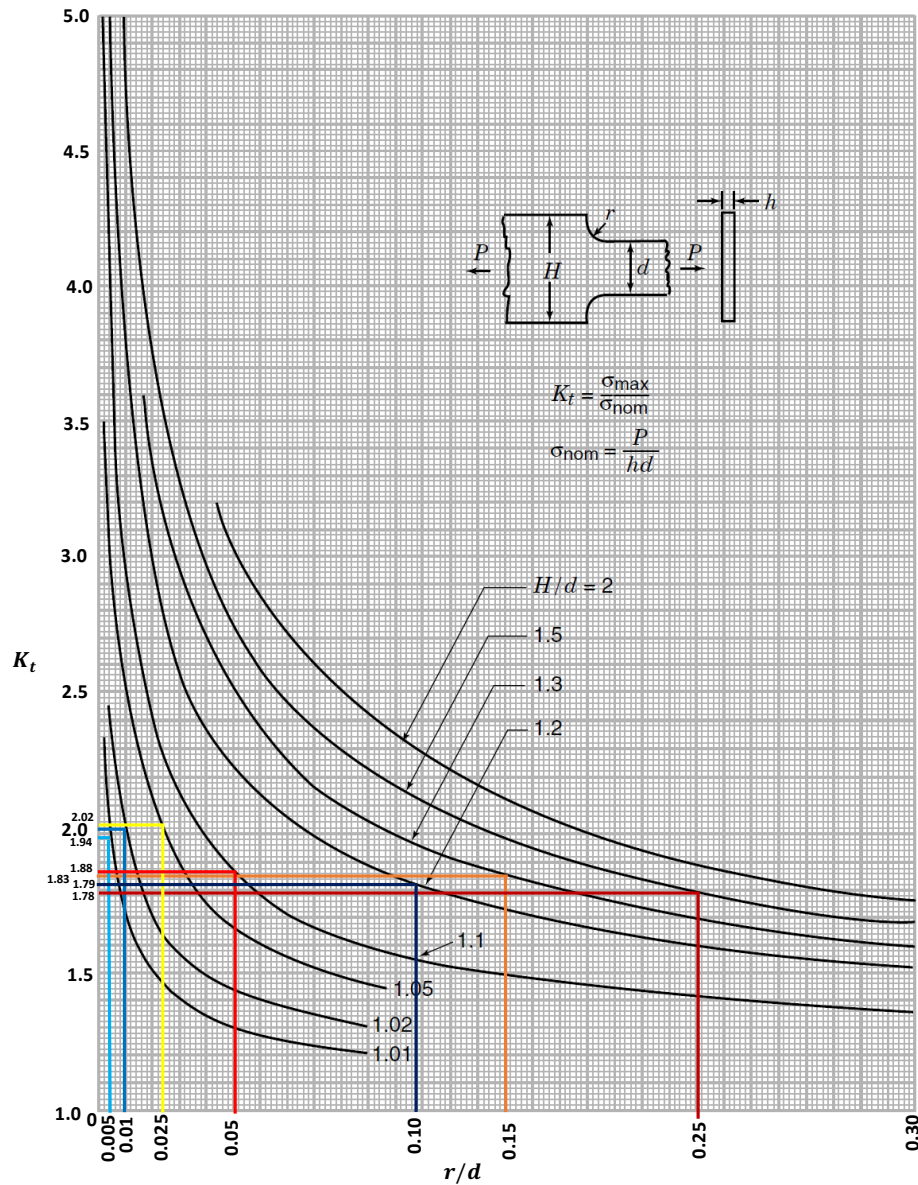

FIGURE 13. A plot of r/d and D/d ratios on a standard graph of Peterson's for axial tension loading [Pilkey W D 1997].

Figure 13 shows the plot of the stress concentration factor (K_t) Vs r/d ratio for different D/d ratios on the standards graph given by Peterson for axial tension loading. In the Peterson graph, 'h' is considered as the thickness of the plate but, in the present study 't' is taken as the thickness of the plate. Authors have obtained a stress concentration factor (K_t) from Peterson's curve for a flat plat presented in Figure 13 for different r/d ratios according to the different D/d ratios. The obtained value of the stress concentration factor (K_t) from the Peterson graph for flat plat is within the range of SCF (minimum to maximum) of the flat plate carried out from the FEA. The derived Rapport factor helps to determine the equivalent stress concentration factor (K_t) for a round bar. The obtained value of the stress concentration factor (K_t) from the Peterson graph is also within the range of SCF (minimum to maximum) of equivalent SCF for a round bar. The values of SCF cannot be found for the D/d ratio equal to 2 and 3 as the range of the r/d ratio is out of the scope of the Peterson curve presented by Peterson (see Figure.13) [Pilkey W D, 1997].

TABLE 11. Average SCF for flat plate, curved plate, equivalent SCF for round bar, SCF from Peterson graph and % variation in SCF

Table No.	D/d ratio	Average SCF for flat plate	Average SCF for curved plate	Average Equivalent SCF for round bar	SCF from Peterson graph	% Variation in SCF (between average SCF for curved plate and round)	% Variation in SCF (between equivalent SCF for round bar and from Peterson graph)
2	1.01	2.279	2.087	2.128	1.94	1.93	8.83
3	1.02	2.268	2.073	2.116	2.00	2.03	5.48
4	1.05	2.191	2.016	2.053	2.02	1.80	1.61
5	1.1	2.109	2.060	2.091	1.89	1.48	9.61
6	1.2	1.468	1.731	1.735	1.78	0.23	2.52
7	1.3	1.871	1.799	1.799	1.83	0.00	1.69
8	1.5	1.721	1.832	1.835	1.79	0.16	2.45
9	2.0	1.527	1.640	1.640	-	0.00	-
10	3.0	1.272	1.420	1.420	-	0.00	-

Table 11 includes the average SCF for flat plate, curved plate, equivalent SCF for round bar, and SCF from the Peterson graph, % variation in SCF (between average SCF for curved plate and round bar) and % variation in SCF (between equivalent SCF for round bar and SCF obtained from Peterson graph). The % variation in the SCF between average SCF for curved plate and round bar, as well as % variation in the SCF between equivalent SCF for round bar and SCF obtained from Peterson graph, are identical.
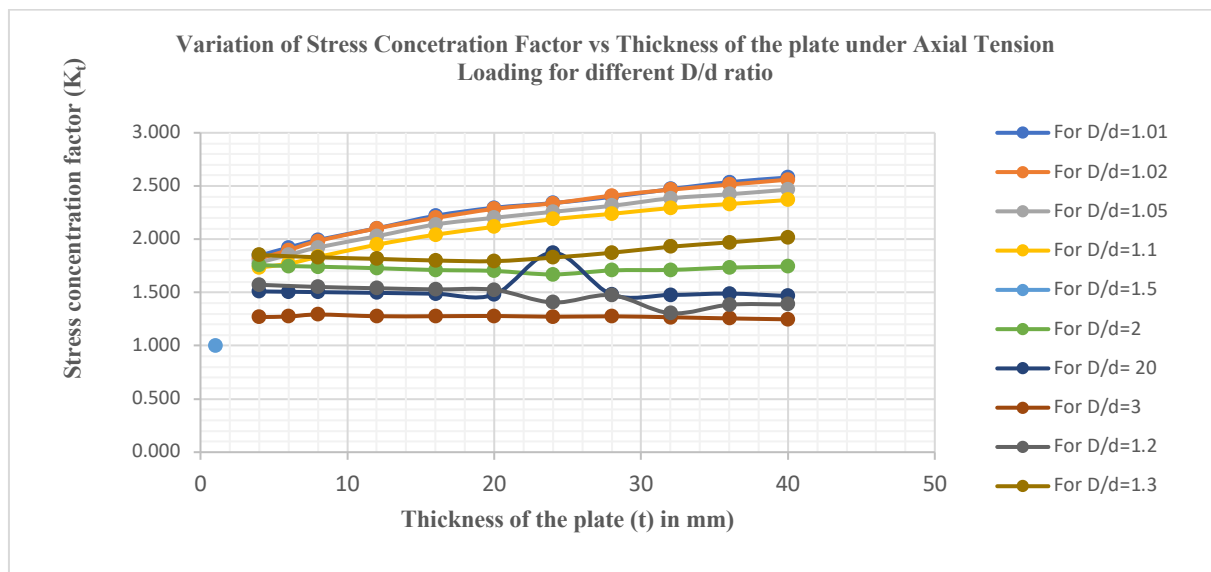

FIGURE 14. SCF vs. Thickness of the flat plate under axial tension loading for different D/d ratios.
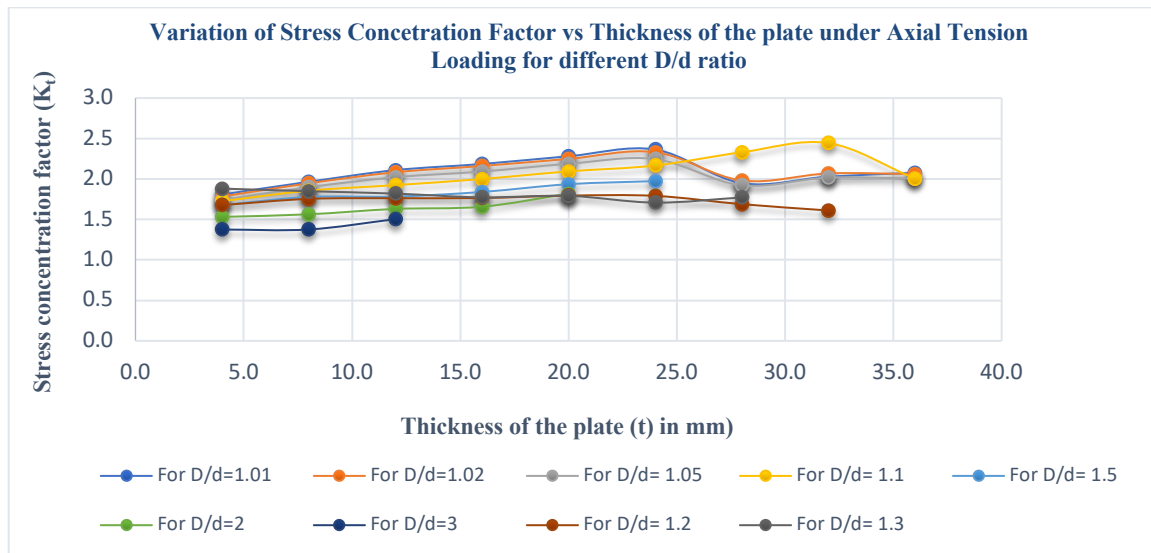
FIGURE 15. Variation of SCF vs. Thickness of the curved plate under axial tension loading for different D/d ratios.

In the present study, the authors have also studied the effect of plate thickness on the stress concentration factor for a flat and curved plate for different D/d ratios. The effect of plate thickness on SCF for different D/d ratios is presented in Figures 14 and Figure 15. The study shows that the SCF is increased as the plate thickness increases.

CONCLUSIONS

The following conclusions were drawn based on the study conducted:

1. The experimental method has limitations to determine the stress concentration factor (SCF) for the shoulder fillet round bar (step shaft) due to the curved surface of the round bar. Also, the fringe pattern is not visible due to the curved surface of the round bar.

2. The fringe pattern is also not visible in the case of partial and full slicing of shoulder fillet round bar due to the problem associated with tooling (narrow tool shape) in buffing operation. Buffing operation is an essential step to prepare the workpiece to perform experimentation.

3. The FEA was performed on a flat plate and curved plate. The effect of the curvature of a curved plate is derived in the form of the Rapport factor by performing FEA on the curved plate concerning the flat plate. The derived Rapport factor is the multiplying factor that helps to determine the equivalent SCF for a round bar with given D/d ratios.

4. The % variation in the SCF is about 2.00 % between the average SCF for curved plates and round bars. The % variation in the SCF is less than 10% between the equivalent SCF for the round bar and SCF obtained from the Peterson graph. Here, both % variations are less than 10%, and it is acceptable variation as per contemporary industrial practices.

5. The SCF has increased minutely as the thickness of the shoulder fillet flat and curved plate increases for the same D/d ratio. The effect of plate thickness on the SCF is very small in the context of thickness variation.

DECLARATION OF COMPETING INTEREST

None

REFERENCES

Allison, I. M. 1961. The elastic stress concentration factors in shouldered shafts PART I: Shafts subjected to Torsion. *The Aeronautical Quarterly*, pp.189 -199. DOI: https://doi.org/10.1017/S0001925900002043.

Allison, I. M. 1961. The elastic stress concentration factors in shouldered shafts PART II: Shafts Subjected to Bending. The Aeronautical Quarterly, pp.219 -227.

Allison, I. M. 1961. The elastic stress concentration factors in shouldered shafts PART III: shafts subjected to axial load. The Aeronautical Quarterly, pp.129 -142. DOI:https://doi.org/10.1017/S0001925900002341.

Andrea Sorrentino, Davide Castagnetti, Andrea Spaggiari & EugenioDragoni. 2019. Shape optimization of the fillet under a bolt's head. *The Journal of Strain Analysis for Engineering Design* 54(4): 247, 253. DOI: 10.1177/0309324719859111. ANSYS workbench 19.0.

Ashish Patel & Chaitanya K. Desai. 2020. Stress concentration around an elliptical hole in a large rectangular plate subjected to linearly varying in-plane loading on two opposite edges. *Theoretical and Applied Fracture Mechanics*106(4). DOI:https://doi.org/10.1016/j.tafmec.2019.102432.

Augusto Ajovalasit, Vincenzo Nigrelli, Giuseppe Pitarresi & Gabriele Virzi Mariotti. 2014. On the history of torsional stress concentrations in shafts: From electrical analogies to numerical methods. *The Journal of Strain Analysis for Engineering Design* 49(6):452-466. DOI: 10.1177/0309324714530123.

Bhavesh Patel & Hiren Prajapati. 2018. Investigation of optimum stress concentration factor for shoulder fillet in round bar under different loading conditions. *Trends in Mechanical Engineering & Technology* 8(2): 18–26.

Collins, J. A. 1981. *Failure of Materials in Mechanical Design: Analysis, Prediction, Prevention*. John Wiley & Sons.

David Taylor et al. 2011. The variable-radius notch: Two new methods for reducing stress concentration. Engineering Failure Analysis pp.1009-1017. DOI: 10.1016/j.engfailanal.2010.12.012.

Design Data. 2010. Data book of Engineers. PSG College of Technology. Coimbatore-641037, Kalailathir Achchagam Publication. Reprint January. DOI: https://doi.org/10.1017/S0001925900002079.

Gyoko Oh, Takumi Sasaki & Yoshiaki Akiniwa, 2020. Experimental and computational analyses on fatigue fracture and microstructure in dissimilar metal weldments with circular sharp stress raiser. *International Journal of Fatigue* 133(4). DOI:https://doi.org/10.1016/j.ijfatigue.2019.105422.

Hartman, J. B. & Leven, M. M. 1950. Factors of stress concentration for the bending case of fillets in flat bars and shafts with a central enlarged section. Society's spring meeting in Cleveland, Ohio, May 27. https://docplayer.net/38040662-Shigley-s-mechanical-engineering-design-tutorial-3-13-stress-concentration.html.

Michele Zappalorto et al. 2014. An engineering formula for the stress concentration factor of orthotropic composite plates. Composites, pp. 51-58. DOI: http://dx.doi.org/10.1016/j.compositesb.2014.08.020.

Mingchao Ding, Yuanliang Zhang, Huitian Lu & Yuan Sun. 2021. Numerical investigation on stress concentration of surface notch on blade. Engineering Failure Analysis. 122(4). DOI:https://doi.org/10.1016/j.engfailanal.2021.105241.

Muminovic, A. J. et al. 2013. Analysis of stress concentration factors (SCF) using different computer software solutions. Procedia Engineering, pp. 609-615. DOI: 10.1016/j.proeng.2014.03.033.

Norton, R. L. 2006. Machine design: An Integrated Approach. Third Edition, Pearson Education. Upper Saddle River, NJ.

Ould Ouali M., Poorsolhjouy, P., Placidi, L. & Misra, A. 2021. Evaluation of the effects of stress concentrations on plates using granular micromechanics. Construction and Building Materials 290(5). DOI:https://doi.org/10.1016/j.conbuildmat.2021.123227.

Pedersen, N. L. 2010. Stress concentrations in keyways and optimization of keyway design. *The Journal of Strain Analysis for Engineering Design.* 45(8): 593-603. DOI: 10.1243/03093247JSA632.

Pedersen, N. L. 2018. Aspects of stress in optimal shaft shoulder fillet. *The Journal of Strain Analysis for Engineering Design* 53(5): 285-294. DOI: 10.1177/0309324718763514.

Pedersen, N. L. 2019. Stress concentration and optimal design of pinned connections. *The Journal of Strain Analysis for Engineering Design* 54(2):95-104. DOI: 10.1177/0309324719842766.

Pilkey, W.D. 1997. Peterson's stress concentration factors. Third Edition, John Wilkey. New York.

Shigley, J. E. & Michke, C. R. 2008. Mechanical engineering design. Eighth Edition, (Tata McGraw Hill, New Delhi, India). pp. 105 & 210.

Sonmez, F. O. 2009. Optimal shape design of shoulder fillets for flat and round bars under various loadings. proceedings of the Institution of Mechanical Engineers. *Part C: Journal of Mechanical Engineering Science* 223: 1741-1754. DOI: 10.1243/09544062JMES1457.

Zappalorto, M. & Lazzarin, P. 2010. Stress fields due to inclined notches and shoulder fillets in shafts under torsion. *Journal of Strain Analysis* 46(3):187-199. DOI: 10.1177/0309324710396019.

Zhihua Xiong, Chenyu Zhao, Yuqing Liu & Haohui Xin Yang Meng. 2021. Biaxial stress concentration of pultruded GFRP perforated plate considering anisotropic factor. Structures 33(10). DOI: https://doi.org/10.1016/j.istruc.2021.06.035.